THREE-PHASE FEEDING SYSTEM FOR RURAL ELECTRIFICATION

Tiago D. C. Busarello, Joselito A. Heerdt, Alessandro L. Batschauer and Marcello Mezaroba.

Electric Power Processing Group - nPEE
Santa Catarina State University - UDESC
Campus Universitario, s/n, PO BOX 89223-100, Joinville, SC, Brazil
mezaroba@joinville.udesc.br

***Abstract* – This paper shows a three-phase feeding system to rural areas that are supplied by a single-phase feeder. This proposed system allows the use of three-phase agricultural equipments. The system proposed is formed by two bidirectional three-phase PWM converters, easily found to acquire at local market. The energy processed by single-phase transformer is maximized due the use of the Power Factor Correction technique at the input converter. The output voltages are free of harmonics and allow non-balanced loads. The control strategy and design procedure are presents to both rectifier and inverter stages. Finally, will be present the experimental results of the proposed feeding system.**

***Key-words* – Single-phase to three-phase conversion, rural feeding systems, back to back converter.**

I. INTRODUCTION

Part of world population lives on rural regions, far away from generation plants and with low population density. The supplying of electrical energy in these regions is usually made by single-phase feeders with single-wire and earth return. Due to this fact, the proprietors are limited to use only single-phase agricultural equipments. To make possible the use of three-phase equipments starting from one-phase electrical source, many researchers have proposed the use of single-phase to three-phase conversion using static converters.

The most popular technique is the use of a single-phase full-bridge diode rectifier with capacitive filter follow by a three-phase inverter with a LC filter. This topology presents the following drawbacks: low power factor and high harmonic distortion on input current, DC bus voltage not regulated and the rectifier is not reversible. In this case, to guarantee low harmonic distortion and a high power factor on input could be used LC passive filters, but this solution results in high weight and volume.

Other possibility to the input stage is the use of a single-phase Boost rectifier with power factor correction. The advantages of this topology are the high power factor on input and a regulated voltage DC bus. The disadvantage is the high current stress in switch that processes all output power.

Aiming the cost reduction, some works proposed topologies that use only two legs to make the conversion, decreasing the number of the switches. These solutions usually uses especial PWM control techniques that need high performance digital microprocessors to implement the control algorithm.

This work presents a single-phase to three-phase converter using a back to back three-phase PWM converter. The input current is equality divided by the three legs of the input PWM controlled rectifier, which operates with high power factor and bidirectional power flux. The choice of reversible converter allows the energy regeneration during transient-load operation and improves the DC link regulation. The output stage of the converter is responsible to generate the four-wire three-phase sinusoidal output voltages.

II. CONVERSION SYSTEM PROPOSAL

The proposed system can be shown in Fig. 1 and is composed by a single-wire earth return isolated feeder and two three-phase PWM converters connected by a DC bus with central tap connected to neutral wire. The rectifier is responsible to ensure unity power factor, improving the power capacity of the single-phase transformer. The input current is divided equally on three branches, reducing the current stresses in the switches and makes possible the use of commercial power modules. The three divided input currents have the same amplitude and angle, and the control principle is similar to three single-phase independent rectifiers.

The output three-phase inverter has three LC filters and provides sinusoidal voltages to output. The central tap of DC link is connected to output neutral and allows the operation of unbalanced loads. The control principle is independent to three phases.

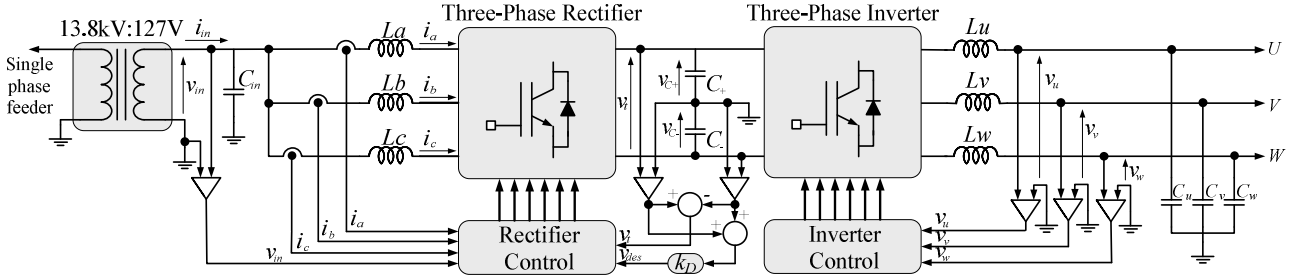

Fig. 1. Conversion System Block Diagram

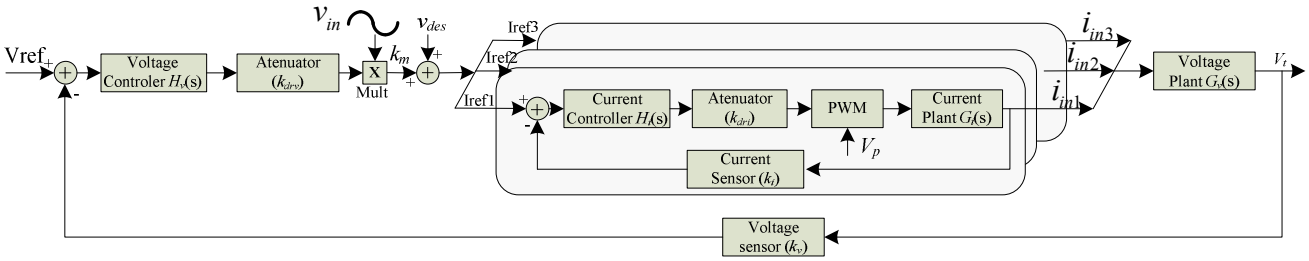

Fig. 2. Control block diagram

The main features of conversion system proposal are: high power factor on input, output regulation and unbalanced load operation.

III. THREE-PHASE RECTIFIER DESIGN

The three-phase current rectifier design is divided in two parts: power design and control design.

A. Power circuit design

To minimize the cost of prototype implementation, the power specifications was made to about 20% of real system. The rectifier power specifications are present on Table 1.

Table 1 - Rectifier power design specifications

Maximum output power	P_o =3,000W
Input voltage	v_{in} = 127V
Total DC bus voltage	v_t =450V
Utility frequency	f_r=50Hz / 60Hz
Switching frequency	f_s=20kHz
Efficiency	η=0.9
Maximum input current ripple	Δ_i=0.27%
Maximum output voltage ripple	Δ_{vi}=1%

The input inductors are calculated by (1) [10].

$$L = L_a = L_b = L_c = \frac{3 \cdot \eta \cdot \left(\sqrt{2} \cdot v_{in}\right)^2 \cdot \left(2 \cdot v_t - 3 \cdot \sqrt{2} \cdot v_{in}\right)}{4 \cdot f_s \cdot \Delta_i \cdot v_t \cdot P_o} \quad (1)$$

Equation (2) shows how to obtain the DC link capacitances [10].

$$C = C_+ = C_- = \frac{P_o \cdot \left(2 \cdot v_t - 3 \cdot \sqrt{2} \cdot v_{in}\right)}{2 \cdot f_s \cdot {v_t}^2 \cdot \Delta_v \cdot v_t} \quad (2)$$

The values obtained from design are 2.74mH for input inductor and 29.7µF for each DC bus voltage capacitor.

Due to availability was used a Semikron BCU+B6I+E1F 3.7kW Power Module. This module has an internal 1,500µF/250V bank capacitor.

B. Control circuit design

The control block diagram of three-phase rectifier can be shown in Fig. 2. The control scheme used was the conventional average current-mode control. This control method is very used in applications like this, mainly when the control implementation is made with analogical circuits. The control is composed by one voltage loop and three current loops. The output of voltage controller is multiplied by a sample of the input voltage and its result is the reference to the current controls. A voltage unbalance compensation circuit was used to guarantee the symmetrical voltage in output capacitors.

The three current loops works in a identical way, the current controllers forces the currents to follow its references, in-phase with the input voltage. The voltage controller regulates the output voltage increasing or decreasing the amplitude of current references.

B.1) Current control design

The open-loop current transfer function is given by (3), and is composed by current plant and the gains of current sensor, PWM modulator and attenuator [10].

$$OLTF_i(s) = \frac{v_t}{3 \cdot L \cdot s} \cdot \frac{k_i \cdot k_{dri}}{V_P} \quad (3)$$

Where:
K_i=0.44 – Current sensor gain;
k_{dri}=0.64 – Attenuator gain located after current controller;
V_p=10 – Triangular carrier amplitude.

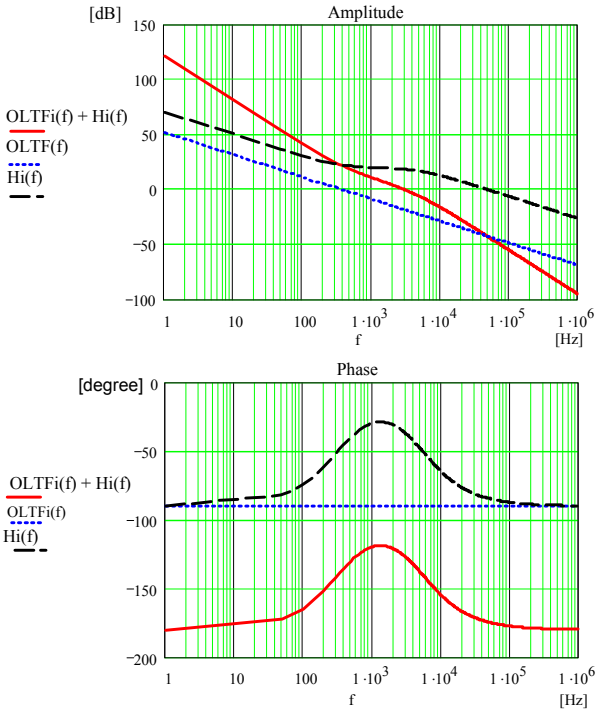

Fig. 3. Bode diagram of OLTFi and controller

Analyzing the equation (3) it's possible to verify the system has a pole located at origin. The current control uses a fast leak and leg controller and its cut-off frequency is 3.3 kHz. The phase margin must be between 30° and 90°. The main parameters of controller are shown in Table 2. The attenuator gain k_{dri} limits the maximum duty-cicle.

Table 2 - Controller parameters

Zero-Crossing frequency	f_{cd}=3.33 kHz
Zero frequency	f_{zd}=333.33 Hz
First pole frequency	f_{p1}=0 Hz
Second pole frequency	f_{2d}=5 kHz
Phase margin	30°<PM<90°

The current controller transfer function is given by (4).

$$G_{ci}(s) = \frac{1 + s \cdot 4.7 \cdot 10^{-4}}{s \cdot 5.03 \cdot 10^{-5} \cdot \left(1 + s \cdot 3.08 \cdot 10^{-5}\right)} \quad (4)$$

Fig. 3 presents the Bode diagram of module and phase of current control. Note that phase margin is about to 50°, satisfying the project requirements.

B.1) Voltage controller design

The voltage control chosen was a PI control and its cut-off frequency is 12Hz. This control should have a low response to ensure the decoupling between the voltage and current controls. The open-loop voltage transfer function is given by (5), and is composed by voltage plant and the gains of voltage sensor, attenuator, multiplier and current sensor.

$$OLTF_{v1}(s) = \frac{3 \cdot v_t \cdot V_p}{2 \cdot P_o} \cdot \frac{1}{\left[s \cdot \frac{C \cdot v_t^{\,2}}{P_o} + 1 \right]} \cdot \frac{k_v \cdot k_m \cdot k_{drv}}{k_i} \quad (5)$$

Where:
k_v=0.01 – voltage sensor gain;
k_m=0.5 – multiplier gain;
k_{drv}=0.25 – attenuator gain located after voltage controller.

By (5) it's possible to verify that the transfer function has only one pole and does not located on origin, causing a static error that should be corrected by controller. The main parameters of voltage controller are shown in Table 3. The attenuator gain k_{drv} limits the maximum input current reference.

Table 3 - Controller parameters

Zero-Crossing frequency	f_{cdt}=12 Hz
Pole frequency	f_{p1}=0 Hz
Zero frequency	f_{zdt}=12 Hz
Phase margin	30°<PM<150°

The transfer function of voltage controller designed is given by (6) [10].

$$G_{cv1}(s) = \frac{1 + s \cdot 12.24 \cdot 10^{-3}}{s \cdot 1.8 \cdot 10^{-4}} \quad (6)$$

Fig. 4 presents the Bode diagram of module and phase of voltage control. Note that phase margin is about to 95°.

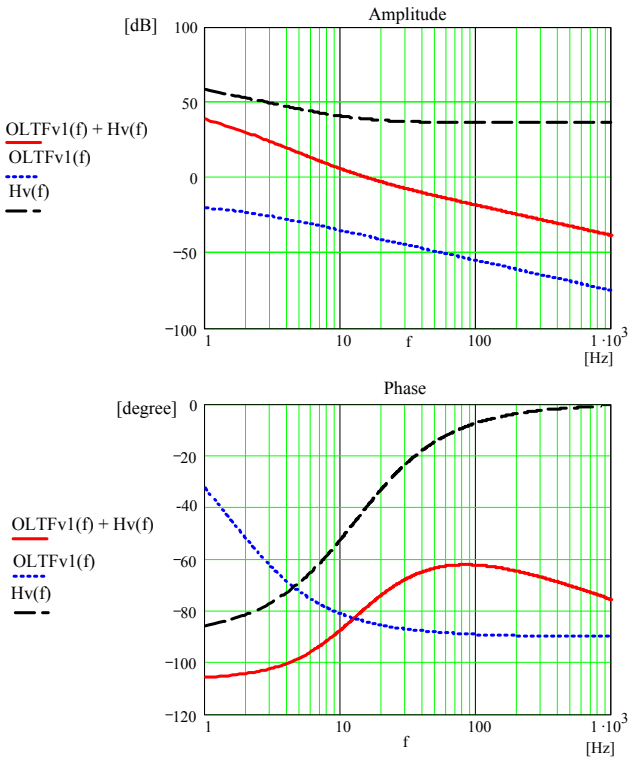

Fig. 4. Bode diagram of OLTFv and controller

IV. THREE-PHASE INVERTER DESIGN

A. Power circuit design

The power circuit is the same used on three-phase current rectifier, but, with a LC filter placed on output. The inverter design specifications are shown on Table 4.

Table 4 - Inverter design specifications

Input voltage	E=450V
Total output power	P_o=2500W
Switching frequency	f_s=20kHz
Filter cut-off frequency	F_o=700Hz
Maximum output current ripple	Δ_{io}=15%

A.1) Filter inductor

The inductance value of output inductor is given by (7) [13]

$$L_o = L_u = L_v = L_w = \frac{v_t}{2 \cdot \Delta_{io} \cdot f_s} \quad (7)$$

A.2) Filter capacitor

The output filter capacitance is given by (8) [13]

$$C_o = C_u = C_v = C_w = \frac{1}{\left(2 \cdot \pi \cdot F_o\right)^2 \cdot L_o} \quad (8)$$

The values obtained of design are L_o=2.75mH to filter inductance and C_o=20µF to filter capacitance.

B. Control circuit design

The control circuit is the same to the three phases, and uses the average voltage-mode control. The control diagram is show on Fig. 5.

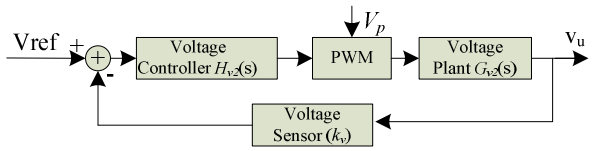

Fig. 5. Control block diagram

The open-loop voltage transfer function is given by (9) and is composed by voltage plant and the gains of voltage sensor and PWM modulator.

$$OLTF_{v2}(s) = \frac{v_t}{L_o \cdot C_o \left[s^2 + \frac{1}{R_o \cdot C_o} \cdot s + \frac{1}{L_o \cdot C_o} \right]} \cdot \frac{kv}{V_p} \quad (9)$$

Where:

k_v=0.025 – Voltage sensor gain;

V_p=10 – Triangular carrier amplitude;

R_o=10k – Open load resistance.

Note that transfer function is composed by two poles located at the same frequency. The controller used is a proportional integral and derivative (PID) and its parameters are shown on Table 5

Table 5 - Controller parameters

Zero cross frequency	f_c=2 kHz
Pole converter frequency	f_o=0.68 kHz
First pole frequency	f_{p1}=0 Hz
Second pole frequency	f_{p2}=13.6 kHz
First zero frequency	f_{z1}=0.68 kHz
Second zero frequency	f_{z2}=0.68 kHz
Phase margin	30°<PM<90°

The transfer function of voltage controller is given by (10) [13].

$$G_{cv2}(s) = \frac{\left(s + 4.54 \cdot 10^3\right)\left(s + 4.63 \cdot 10^3\right)}{\left[s \cdot \left(s + 8.54 \cdot 10^4\right)\right]} \cdot 214.28 \quad (10)$$

Fig. 6 presents the Bode diagram of module and phase of voltage control. Note that phase margin is about to 40°.

V. EXPERIMENTAL RESULTS

The experimental results were obtained at nominal conditions. The results were captured through a digital oscilloscope TPS2024 model by Tektronix®, where has been saved the points and plotted on software MatLab®. The mains experimental results are showed as follow:

Fig. 7 presents input voltage and the input current waveforms with the system operating with nominal load. Note that input current is almost in phase with the input voltage ensuring a high power factor. The small phase-shift between voltage and current input is due the high frequency capacitor filter at input rectifier.

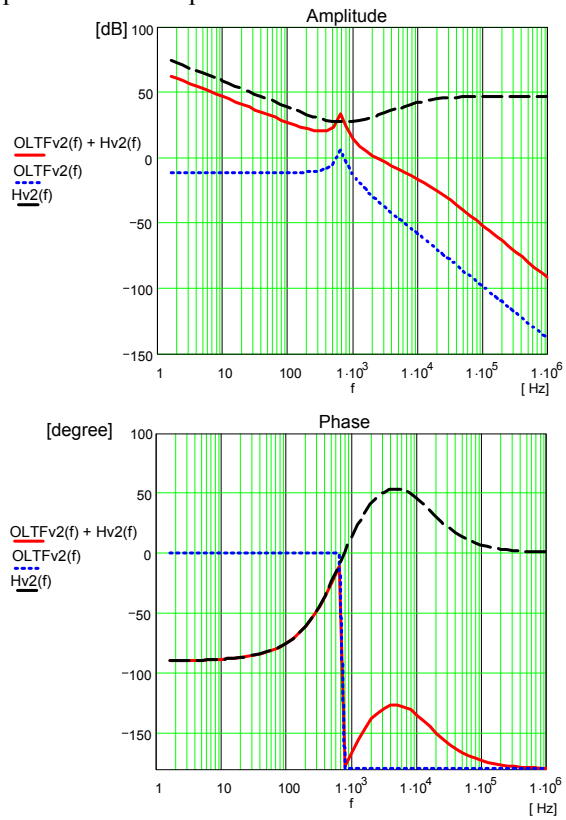

Fig. 6. Bode diagram of OLTFv2 and controller.

Fig. 8 presents the tree divided input currents. It can verify that the current was equally divided through three legs of rectifier.

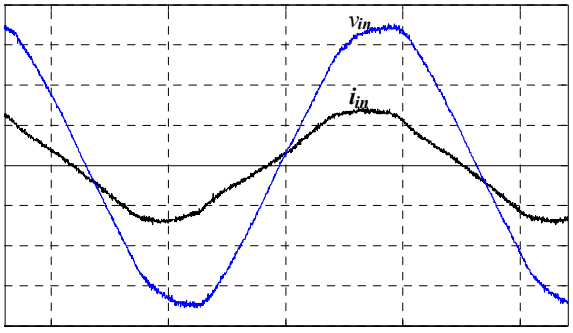

Fig. 7. Input voltage Vin and input current Iin. (50V/div, 25A/div, 5ms/div)

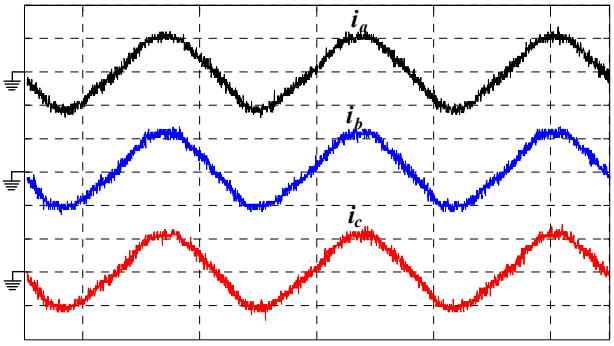

Fig. 8. Current on branches A, B e C (10A/div, 10ms/div)

Fig. 9 presents the half positive, half negative and total DC bus voltage.

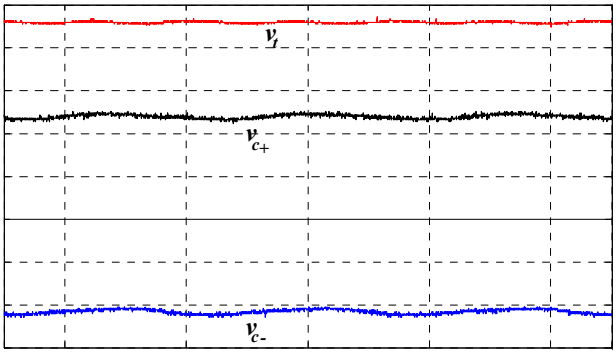

Fig. 9. Positive DC bus voltage (100V/div, 5ms/div)

Fig. 10 presents output voltage waveforms of inverter.

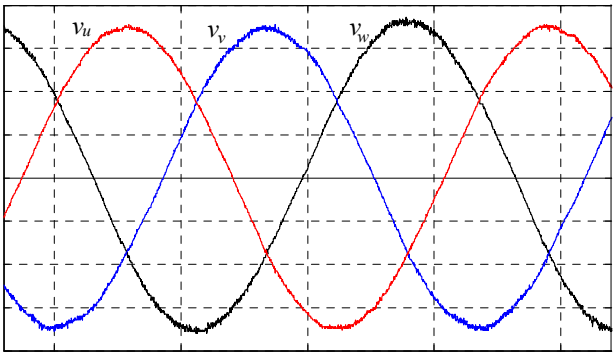

Fig. 10. Output voltage Vu, Vv and Vw. (50V/div, 5ms/div)

Fig. 11 presents the input current behavior and total DC bus voltage behavior during the start-up processing.

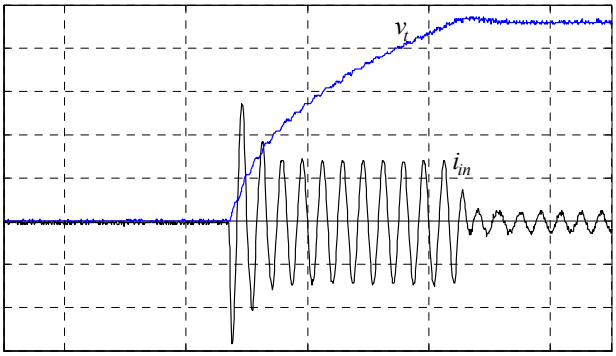

Fig. 11. Total DC bus voltage Vt and input current Iin. (100V/div, 25A/div, 100ms/div)

Fig. 12 presents input current and DC bus voltage during a step of load from10% to 100% nominal load.

Fig. 13 presents the input current and DC bus voltage during a step of load from 100% to 10% nominal load.

Fig. 14 presents harmonic spectral of output voltage. The fundamental harmonic was omitted to better visualization. It can be verify that no harmonics overcome 1% of fundamental. The voltage total harmonic distortion (THD) is approximately 0.94%.

Fig. 15 presents input current harmonic spectral. The fundamental harmonic was omitted to better visualization. The input current total harmonic distortion (THD) is approximately 7.0%.

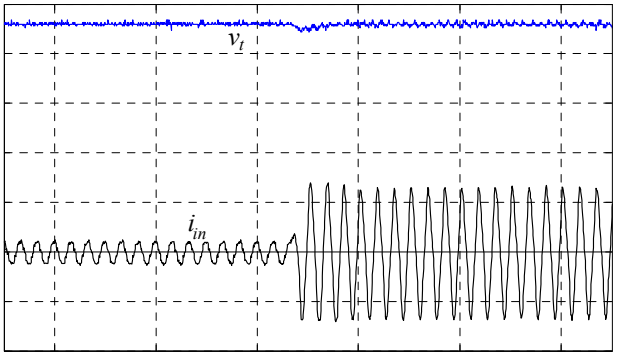

Fig. 12. Total DC bus voltage Vt and input current Iin, setting 100% of load. (100V/div, 25A/div, 10ms/div)

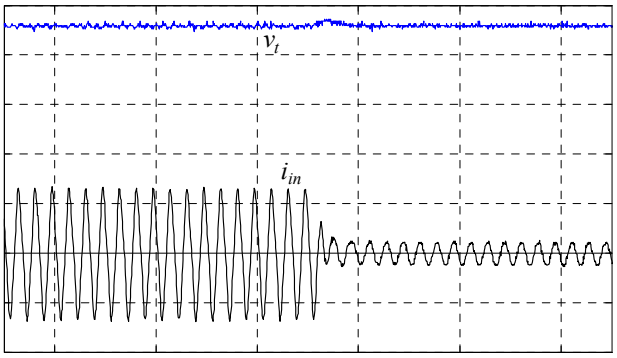

Fig. 13. Input current and total DC bus voltage withdrawal 100% of load. (100V/div, 25A/div, 10ms/div)

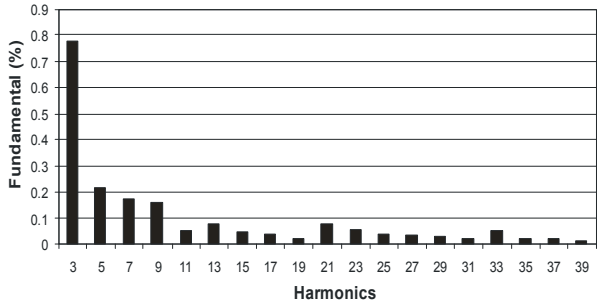

Fig. 14. Output voltage harmonic spectral

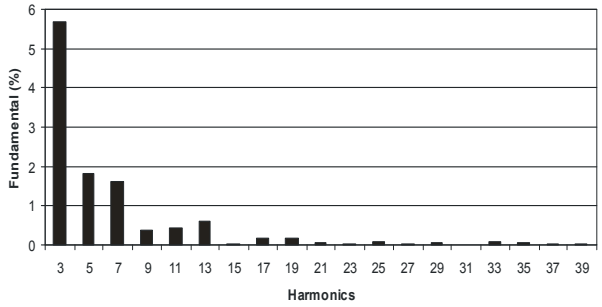

Fig. 15. Input current harmonic spectral

Fig. 16 presents input voltage harmonic spectral. The fundamental harmonic was omitted to better visualization.

The input voltage harmonic distortion (THD) is approximately 2.46%.

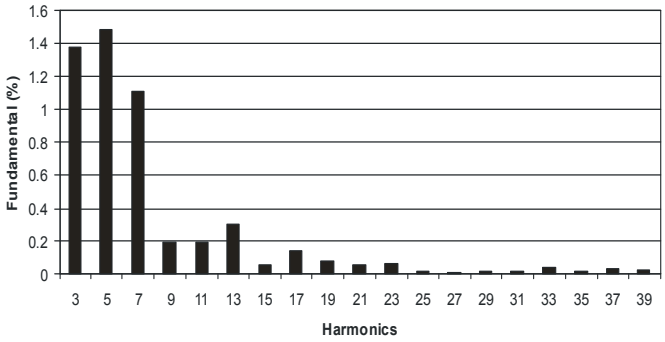

Fig. 16. Input voltage harmonic spectral

Fig. 16 presents the prototype implemented to obtain the experimental results.

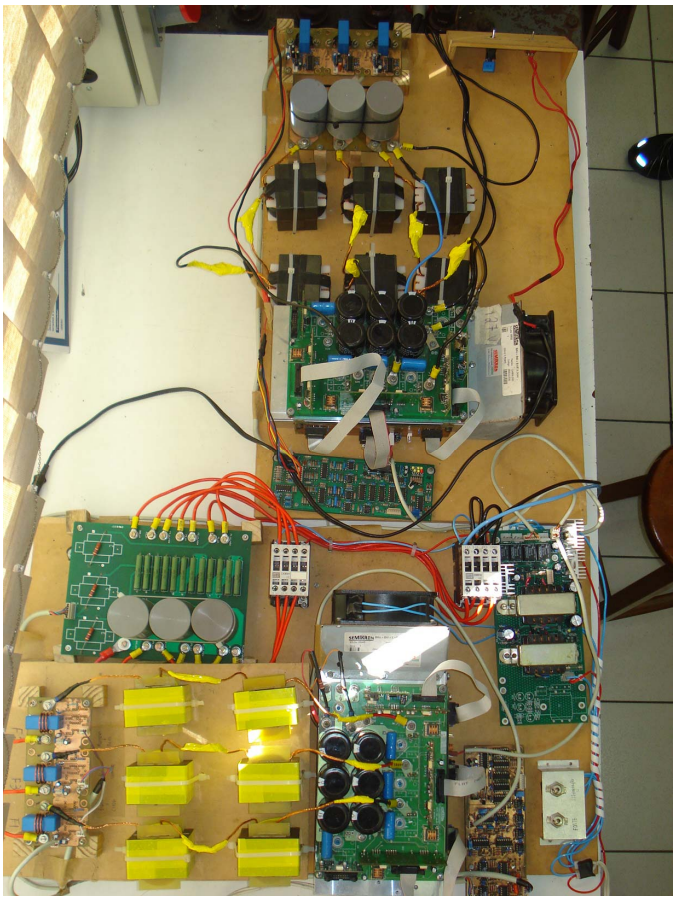

Fig. 17. Prototype implemented

VI. CONCLUSION

The proposed system to realize single-phase to three-phase conversion in rural areas showed a quite attractive solution. Due to use of commercial power module, the converters designs become quite simple.

It was possible verify that input current was divided equally in on three rectifier legs, decreasing the switches stresses. The rectifier presents a high power factor and consequently the power energy processing by the single-phase transformer was maximized.

The control designs to both converters are well-known and the dynamic behavior was very good.

From experimental results it can conclude that the proposal system is very efficient and the design requirements were achieved.

VII. REFERENCES

[1] G. A. Covic, G. L. Peters, J. T. Boys, "An Improved Single Phase to Three Phase Converter for Low Cost AC Motor Drives", *IEEE Catalogue No. 95TH8025.*

[2] R. Q. Machado, S. Buso, J. A. Pomilio, "A Line-Interactive Single-Phase to Three-Phase Converter Sytem", *IEEE Transaction on Power Electronics, Vol 21, NO. 6, November 2006.*

[3] P. Enjeti, S. A. Choudhury, "A Low Cost Single Phase to Three Phase Static Power Converter", *IEEE Transaction, Paper No. 92 A4, 1992.*

[4] S. B. Bekiarov, A. Emadi, "A New On-Line Single-Phase to Three-Phase UPS Topology with Reduced Number of Switches", *IEEE Transaction, 2003.*

[5] P. Enjeti, A Rahman, "A New Single Phase to Three Phase Conveter with Input Current Shaping for Low Cost AC Motor Drives", *IEEE Transaction, 1990*

[6] E. N. Tshivhilinge, M. Malengret, "A Practical Control of a Cost Reduced Single Phase to Three Phase Converter ", *IEEE Transaction, 1998.*

[7] R. S. Ramshaw, J. D. Allan, R. A. Decon, "One-Phase to Three-Phase Conversion Utilizing Forced Phasimg", *IEEE Transactions*, July/August 1990.

[8] I. Barbi, Projeto de Fontes Chaveadas, Autor's Edition, Florianópolis, 2001.

[9] J. C. RAYCIK, "Projeto de um Retificador de Corrente Reversível com Alto Fator de Potência Implementado em DSP", *Master of Science Thesis*, LEPO, UDESC,

[10] F. L. Cardoso, "Projeto de um Retificador Bidirecional com Alto Fator de Potência com Controle por Valores Médios Instantâneos Implementado no DSP TMS320F2812", *Master of Science Thesis*, LEPO, UDESC, Joinville, SC, 2006.

[11] R. Stoicescu, K. Miu, C. O. Nwankpa, D. Niebur, X. Yang, "Three-Phase Converter Models for Unbalanced Radial Power-Flow Studies" *IEEE Transactions on Power System,* Vol. 17, No. 4, November 2002.

[12] N. Mohan; T. M. Undeland; P. W. Robbins; "Power Electronics: Converters, applications and Design"; John Willey & Sons; Singapore, 1989.

[13] J. D. Sperb, "Projeto de um Inversor Trifásico com Snubber de Undeland Regenerativo e Controle Digital Implementado no DSP TMS320F2812", *Master of Science Thesis*, LEPO, UDESC, Joinville, SC, 2006.

VOLTAR